As-Fab Elements – Design vs. Reality

By Victor E. Densmore*

A Masters Report Submitted to the Faculty of the

COLLEGE OF OPTICAL SCIENCES

In partial fulfillment of the requirements for the degree of

Master of Science in Optical Sciences

In the Graduate College of

The University of Arizona

December 2018

- The research presented herein was done with the help of Ruda Cardinal Inc. staff: Christopher M. Shanor, Isela D. Howlett, Kate Medicus, Tilman Stuhlinger, and Kenneth R. Castle who are co-authors in the published paper resulting from this work presented at SPIE 2018 [5]

Table of Contents

1. INTRODUCTION 3

1.1 Hypothesis 4

1.2 The Parts 4

1.3 Tolerancing Irregularity in Optical Modeling Software 6

1.4 Definition of Terminology 10

2. Measured Irregularity Results 12

2.1 Spherical vs. Astigmatism 12

2.2 Other aberrations 14

2.3 PV and rms 17

2.4 R/# Impact 19

2.5 Lens Aspect Ratio Impact 20

3. Future work 24

4. Conclusions 21

ACKNOWLEDGEMENTS 25

REFERENCES 25

1. INTRODUCTION

The use of raytracing software is commonplace in optical engineering and allows the generation and testing of mathematical models by the optical designer. After the optical design is shown to meet necessary performance criteria, a tolerance and sensitivity analysis is often done to consider fabrication and assembly errors that typically cause optical performance degradation. Common assembly errors in optical systems include lens element positional errors and common fabrication errors in the lens radius of curvature, center thickness, and surface irregularities such as astigmatism and spherical. The robustness and manufacturability of the optical design is often qualitatively indicated by the results of the sensitivity analysis and can be statistically modeled by Monte-Carlo analysis.

This report considers the irregularity component of commonly used tolerance analysis and shows how the modeled errors differ from the actual as-fabricated (TIRR) errors. In a typical tolerance analysis, the irregularity is modeled by assuming an equal combination of spherical and astigmatism. But, upon inspecting the measured irregularities for many different lenses, we find instead a dichotomy – either spherical *or* astigmatism errors occur, rather than being equally probable.

The R/# of a surface is used throughout this paper:

R/# $$R/\# = \frac{Surface\ Radius\ of\ Curvature}{Surface\ Aperture\ Diameter}. \quad (1)$$

The relationships between coma and astigmatism, the type of surface (concave, convex, or planar), the relationship between peak-to-valley and root-mean-square errors, the dependence of aberration on R/#, and the dependence of aberration on lens aspect ratio are also considered. Data are gathered from a sample of 1052 surface irregularity measurements on real optical surfaces.

1.1 Hypotheses

A correlation between the type of lens surface figure errors and manufacturing method and/or lens characteristics is expected. Knowing such a correlation between astigmatism and/or spherical irregularities and lens characteristics *a-priori* could allow for more accurate Monte-Carlo analysis.

The hypotheses are:

1) The amount of spherical aberration is not correlated to the amount of astigmatism.
2) Convex and concave surfaces show no correlation between amounts of spherical and astigmatism.
3) Planar surfaces exhibit more astigmatism than spherical aberration.
4) Coma is lower in magnitude and not correlated to astigmatism.
5) There is no correlation between the percentage of spherical, astigmatism, and coma on surface shape.
6) There is a correlation between R/# and the amount of aberration.
7) There is a correlation between lens aspect ratio and the amount of aberration.

1.2 The Parts

The data presented here are from 52 different lens types made with various optical glasses, curvatures, and diameters; multiple quantities (between 7 to 30) of each lens was made, allowing for multiple samples across the wider breadth of data. A total of 1052 surface irregularity measurements are analyzed. The nominal radii of curvature of the spherical lenses ranges from 6.67 mm to 495.88 mm,

and the clear aperture ranges from 6 mm to 36 mm. Plano surfaces are also shown. In general, the irregularity tolerance for these lenses is 0.1 waves peak-to-valley (PV) at 632.8 nm. The optical model analysis shows good performance with a modeled 0.1 wave PV error. Some parts show higher PV values due to different tolerances. There was no specification on higher order aberration terms.

All lenses in this study are fabricated and tested by Optimax Systems, Inc. [1]. All surfaces are CNC ground to approximate shape and subsequently pitch-polished. Radius of curvature and surface irregularity is tested for each lens on a commercially available phase-shifting Fizeau interferometer equipped with a radius scale (with displacement interferometry). Measurement accuracies are understood to be negligible in the current context. Examples of the irregularity measurements are shown in Figure 1, where (a) shows a surface with significant spherical (and higher order terms) error and (b) shows significant astigmatism.

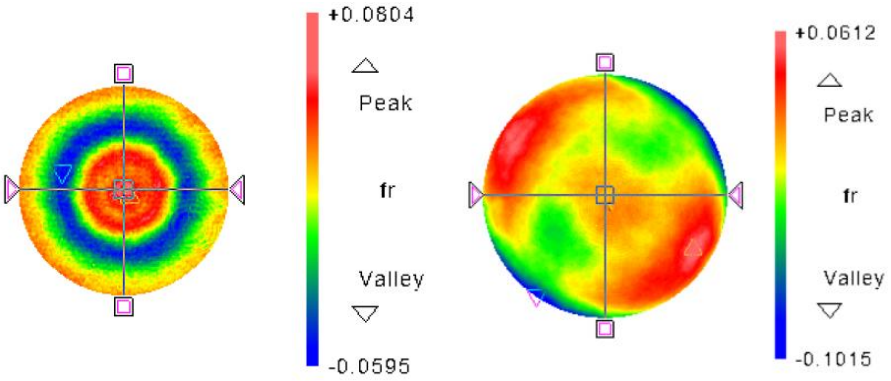

(a) (b)

Figure 1. Two irregularity measurements from the interferometer showing residual spherical (a) and astigmatism (b). A fringe (fr) here indicates 0.5 waves.

It is feasible that the different aberrations are due to different fabrication processes and/or setups. For example, surfaces with large R/# allow for multiple quantities to be fabricated simultaneously on lapping and polishing machines, which is known as a "multiple block". Surfaces with small R/#s are more difficult to fabricate and generally can only be made as singles – one part per tool. In many cases, parts from the multiple block (large R/#s) show more astigmatism than spherical (except for the center component). In contrast, parts from the single block typically show more spherical than astigmatism (small R/#s). These routines help define the hypotheses in section 1.1.

1.3 Tolerancing Irregularity in Optical Modeling Software

There are several different optical design software packages that handle tolerancing and surface irregularity in different ways. In this work, the surface irregularity is modeled in Zemax® and OpticStudio® by using the "TIRR" tolerance. OpticStudio's Help File describes the TIRR irregularity modeling as combination of equal parts spherical and astigmatism [2]. The TIRR command calculates the surface sag error (Δz) for irregularity tolerancing as

$$\Delta z = \frac{\lambda_t W}{4}(\rho^4 + \rho_y'^2), \tag{2}$$

where

$$\rho = \sqrt{(p_x^2 + p_y^2)} \tag{3}$$

and

$$\rho_y' = \rho cos\theta, \tag{4}$$

where ρ_x and ρ_y are the normalized lateral (radial) coordinate on the height map, θ is the angular coordinate, λ_t is test wavelength, and W is the amount of error assumed in the model in fringes.

An example of this irregularity surface sag error from the Zemax analysis is shown in Figure 3. In Figure 3(left), the surface sag, Eqn. 1, is plotted directly for an input W of 0.1 fr (equivalent to 31.6 nm in a standard double pass test in HeNe). The PV of this height map is 32.3 nm. This small difference between the input and the output PV is explained by the pixelization of the height map and is not of concern. What is of concern is shown in Figure 3(right), where the power error (ρ^2) is removed. This power error is removed for multiple reasons: because power error is better represented as a radius error, the interferometer test of the irregularity doesn't measure the power error, and because the surface sag is not normal to the surface, as it should be. The difference between measuring the surface sag along the surface normal versus along a direction, such as an optical axis, is illustrated in Figure 2 below.

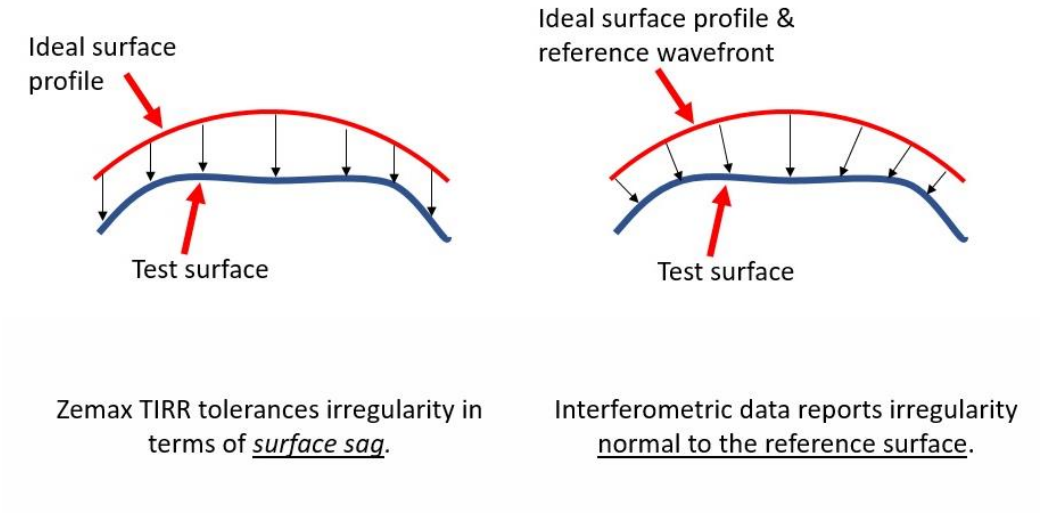

Figure 2: Sag error can be functionally represented as a sag error along an axis (left) but sag error is more naturally measured along the normal to a reference surface or wavefront using an interferometer.

The output PV of this height map is much more representative of the actual measured PV of a surface with the modeled error. The PV of Figure 3(right) is 16.9 nm, which is about half of the input value.

Figure 4 shows this same trend for a range of irregularity (*W*) inputs. In summary, the measured PV will be about half of the modelled PV.

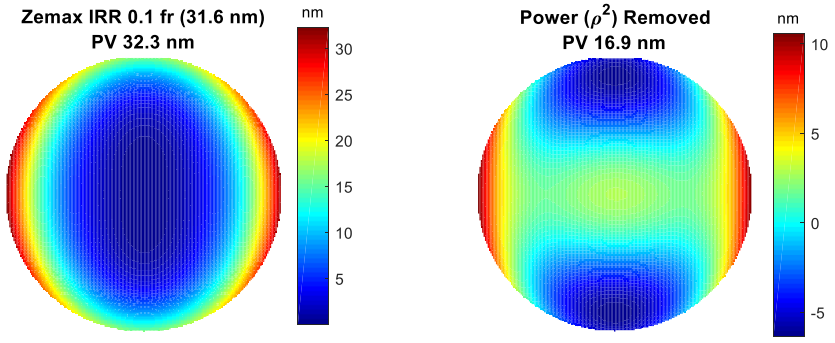

Figure 3: The surface sag error of Eq. (1) with an input of 0.1 fr for *W* (left) and the same surface sag error with the power term removed (right). Power is sometimes called focus or defocus and here means the ρ^2 term mathematically.

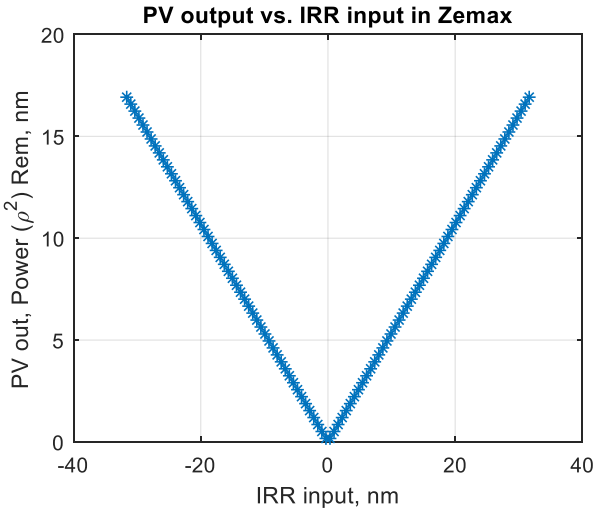

Figure 4: The PV output (after removing power errors) for the Zemax modeled irregularity. Note that the output is about half of the input.

The consequence of using TIRR for specification therefore is a mismatch between the model and the as-manufactured part. For example: an optical designer inputs 0.1 fr as *W* in the TIRR analysis. The

analysis is run with 0.05 fr (because of the typical re-focusing in the model) and the designer determines that the performance meets specification. Then the designer puts the same 0.1 fringes on the optical print for a PV specification thinking that is needed for performance. Then optical manufacturing facility provides a part with 0.1 fr error, which is double what is actually modeled. The parts have more error than is modelled. This discrepancy still holds true for a non-interferometric test because manufacturers typically report irregularity with all power removed.

Perhaps this difference is because optical testing results were historically reported in wavefront, not in surface error. A typical manufacturer now reports irregularity as the surface error, irrespective of the units specified.

This method of tolerancing irregularity (equal spherical and astigmatism) is simplistic, but it is the most commonly used method due to its ease of use. Zemax and other software packages can do more complex irregularity tolerance analysis, where the individual irregularity components (typically Zernike terms) are toleranced separately.

Two points of concern in the default tolerancing are: 1) the use of the Seidel aberrations; and 2) the tolerance error is added through a sag deformation instead of along the surface normal (typical during testing). For the later concern, the first effect is an error in the power (radius of curvature) that becomes larger for smaller R/#s. This power factor is subtracted at this time. There are some secondary effects with spherical and high order spherical terms (again, larger with the smaller R/#s). This effect is noted, but is not considered at this time. Further work could include calculating the magnitude of this error,

but the better solution is to use the more complex irregularity tolerancing in the optical modeling software when the error is along the surface normal.

The use of Seidel aberrations is not recommended because of their non-orthogonally and their mismatch with the more commonly used Zernike aberrations during optical testing. In the interferometric optical test of spherical and plano surfaces (where power is removed), the Seidels are easily converted to the Zernike terms, as shown in section 1.4. Testing results shown below use the more common Zernike terms that have a defined relationship with the Seidels.

1.4 Definition of Terminology

The Zernike aberration definitions used in this paper use the orthogonal, orthonormal set of Zernike polynomials [3] and are:

Zernike Spherical Aberration: $$H_{Sph} = Z_4^0\sqrt{5}(6\rho^4 - 6\rho^2 + 1), \quad (5)$$

Zernike Astigmatism X: $$H_{AstigX} = Z_2^2\sqrt{6}(\rho^2 cos2\phi), \quad (6a)$$

Zernike Astigmatism Y: $$H_{AstigY} = Z_2^{-2}\sqrt{6}(\rho^2 sin2\phi), \quad (6b)$$

Zernike Coma X: $$H_{ComaX} = Z_3^1\sqrt{8}(3\rho^2 - 2)\rho\cos(2\phi), \quad (7a)$$

and

Zernike Coma Y: $$H_{ComaY} = Z_3^{-1}\sqrt{8}(3\rho^2 - 2)\rho\sin(2\phi) \quad (7b)$$

Generally, the absolute value of the Spherical Aberration (S_{40}) is used in the following analysis. Individual Zernike terms are combined in a root-sum-square manner to determine the magnitude of the astigmatism and coma:

Zernike Astigmatism Magnitude: $$Z_2^{2m} = \sqrt{(Z_2^2)^2 + (Z_2^{-2})^2} \quad (8a)$$

and

Zernike Coma Magnitude: $$Z_3^{1m} = \sqrt{(Z_3^1)^2 + (Z_3^{-1})^2} \quad (8b)$$

The conversion between the Seidel and Zernike coefficients is a non-trivial problem. In the case considered here – no power or tilt in the measurements and no higher order Zernike terms considered – the following relationships are made between the Seidel terms (S_{xx}) and the Zernike terms (Z_x^x):

Spherical Aberration: $$S_{40} = Z_4^0\ 6\sqrt{5}, \quad (9a)$$

Astigmatism $$S_{22} = Z_2^{2m}\ 2\sqrt{6}, \quad (9b)$$

and

Coma $$S_{31} = Z_3^{1m}\ 6\sqrt{2}. \quad (9c)$$

The tolerance relationship in the Zemax TIRR analysis assumes a one-to-one ratio between S_{40} and S_{22}. To compare our measured Zernike terms, an update to this relationship is required as follows:

$$\frac{S_{40}}{S_{22}} = 1 = \frac{Z_4^0\ 6\sqrt{5}}{Z_2^{2m}\ 2\sqrt{6}} = 2.7386\frac{Z_4^0}{Z_2^{2m}} \quad (10)$$

The data in Figure 5 show Z_4^0 plotted versus Z_2^{2m}. To compare this measured data to the Zemax analysis, we will plot $Z_4^0 = 0.365 * Z_2^{2m}$ as calculated from equation (10) [2-3].

2. MEASURED IRREGULARITY RESULTS

The following sections show data of the as-fabricated lenses in various forms look for trends and compare to the optical modeling software. Most data shows the data sorted by surface type – concave (CC), convex (CX), or plano. All optical surfaces are measured using a commercially available Fizeau interferometer by Optimax. All data has tilt and power removed. Some analysis shows Zernike polynomials (1.4), which are used to examine specific aspects of surface irregularity. The PV numbers shown here are full PV in the part's clear aperture. While PVr [4] or PV99 (masking the lowest and highest data points) are typically better values, these values not available at the time of this writing.

2.1 Spherical vs. Astigmatism

The plots for spherical vs. astigmatism are shown in Figure 5. Spherical aberration, |SA|, is defined by the absolute value of Eq. (9), and astigmatism is defined by Eq. (8a). The Zemax irregularity model ($Z_4^0 = 0.609 * Z_2^{2m}$) is shown as the red line. Clearly the data do not follow the trend of the Zemax model. The blue line shows a linear trend of the data. It is clear that the data does not fit well to a linear trend.

There appears to be a tradeoff for concave surfaces between the astigmatism and spherical terms, as suggested by the more triangular grouping of data points. This is the either spherical or astigmatism being the dominating error, as listed in hypothesis #1. The same story is harder to tell for the convex surfaces. The data does show that plano surfaces are more susceptible to astigmatism than spherical figures errors during the fabrication process, as expected.

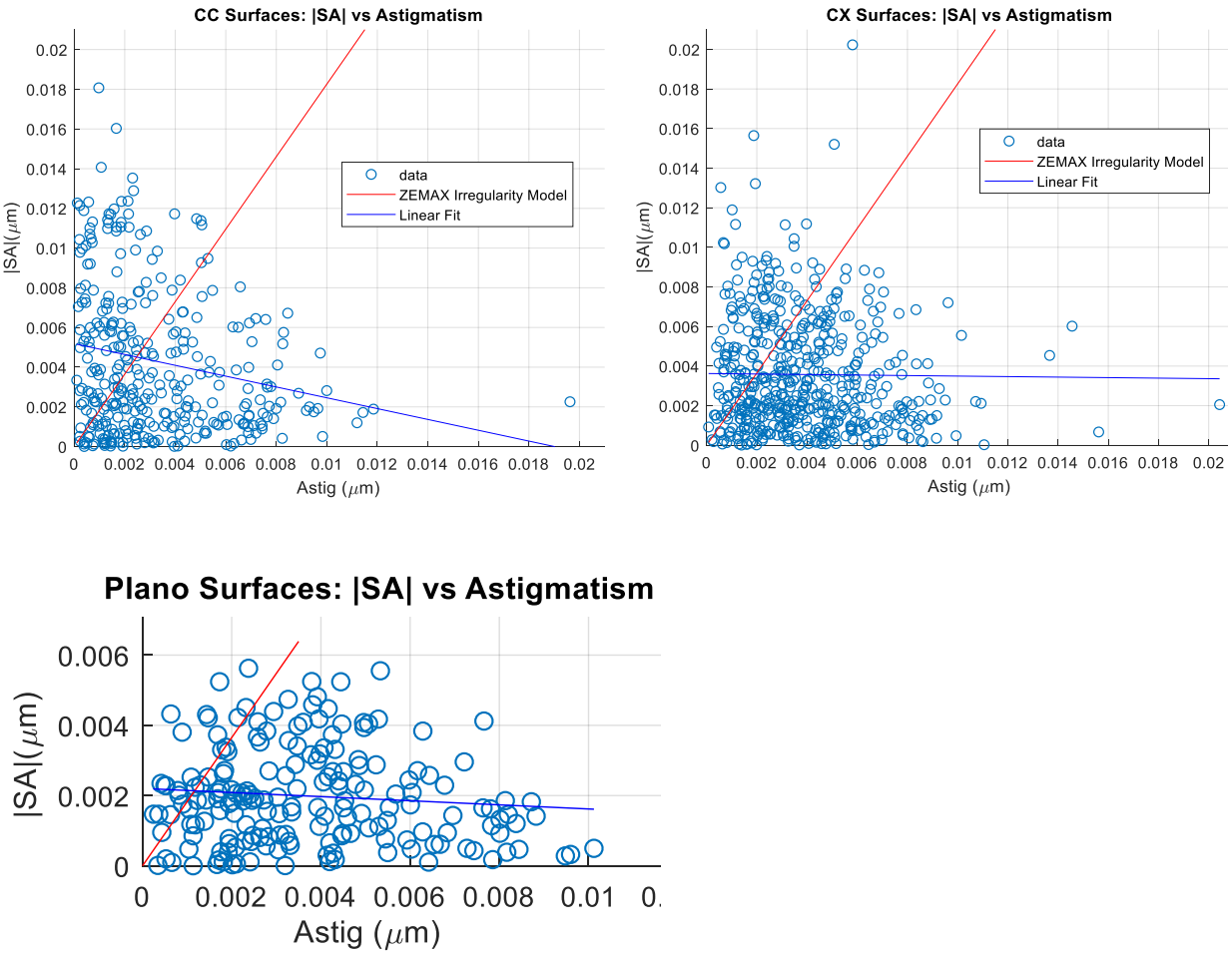

Figure 5. The absolute value of spherical versus astigmatism terms.

Sign of Aberrations

The plots presented here show the absolute value for spherical aberration. When the sign of spherical (vs. astigmatism or vs. R#) is considered, there are no additional conclusions that can be drawn. The sign of the spherical appears to differ when surface shape is considered: 58.7% of the concave surfaces have positive spherical and 49.4% of the convex surfaces had positive. This result is interesting, but there is not enough known about the manufacturing process to determine if this result is due to a

process difference or just a statistical anomaly. Also, the difference is not large enough to force a change in the modeled distribution in the irregularity tolerance model.

The sign of astigmatism, when considering Zernike methods, cannot be separated from the clocking of the aberration. This clocking is not significant to the single-surface analysis in this report.

2.2 Other Aberrations

The standard irregularity model takes only spherical and astigmatism into account. A typical part typically has more components of surface error, but these are not easily represented by simple values. Spherical and astigmatism are notable in that traditional manufacturing processes naturally lend themselves to creating those types of errors. Optical errors like coma are more of an assembly error than a manufacturing error (excepting some sub-aperture polishing processes and aspheres which are not considered here). Even so, the coma terms are plotted versus astigmatism to determine if coma has a more apparent correlation. The data, plotted below in Figure 7, do not suggest any notable relationship. In addition, the magnitude of the coma terms are small compared to the astigmatism and spherical terms.

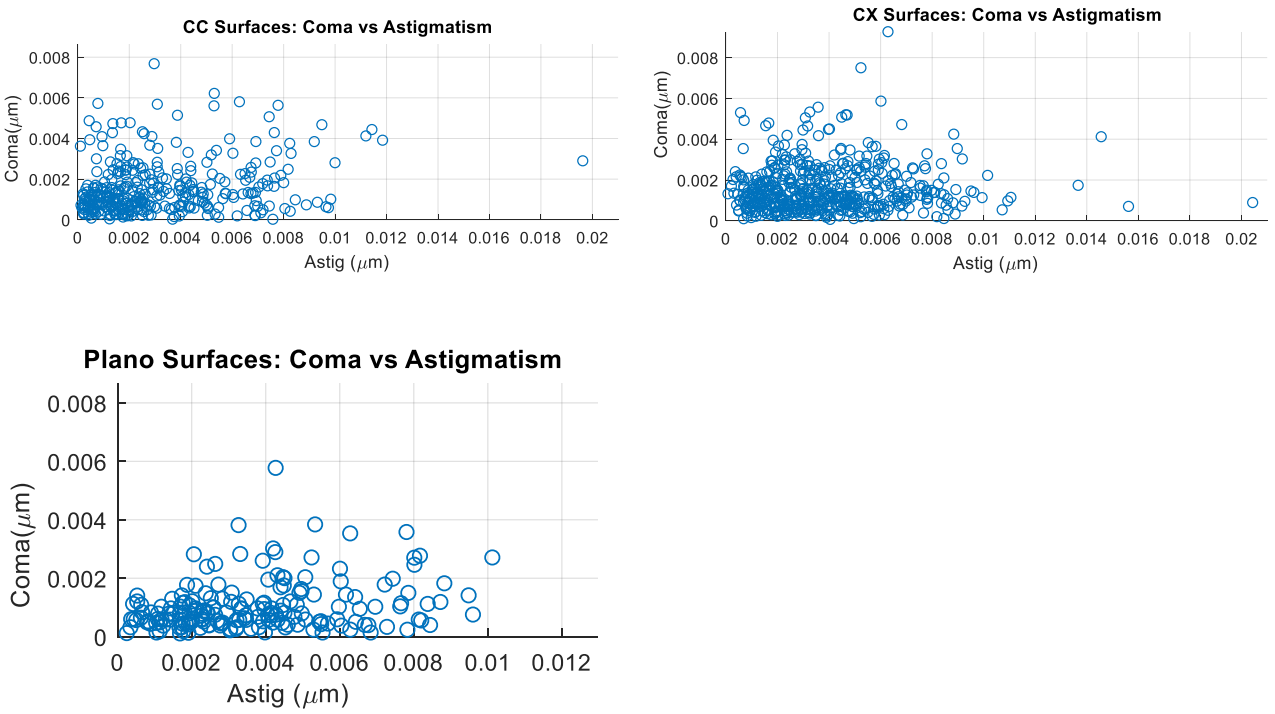

Figure 6. Coma versus astigmatism. These data do not show strong correlations.

Another way to look at this result is to plot the relative amount of aspherical, astigmatism, and coma, as is shown in Figure 7 where the aberration percent for each term is plotted. The aberration percent is:

$$\left(\frac{|Aberration|\ (\mu m)}{PV\ (\mu m)}\right) * 100. \tag{11}$$

As shown, spherical is the dominating error and coma is small. For the plano surfaces, the astigmatism is a larger contributor to the PV as compared to the CC and CX surfaces, as expected.

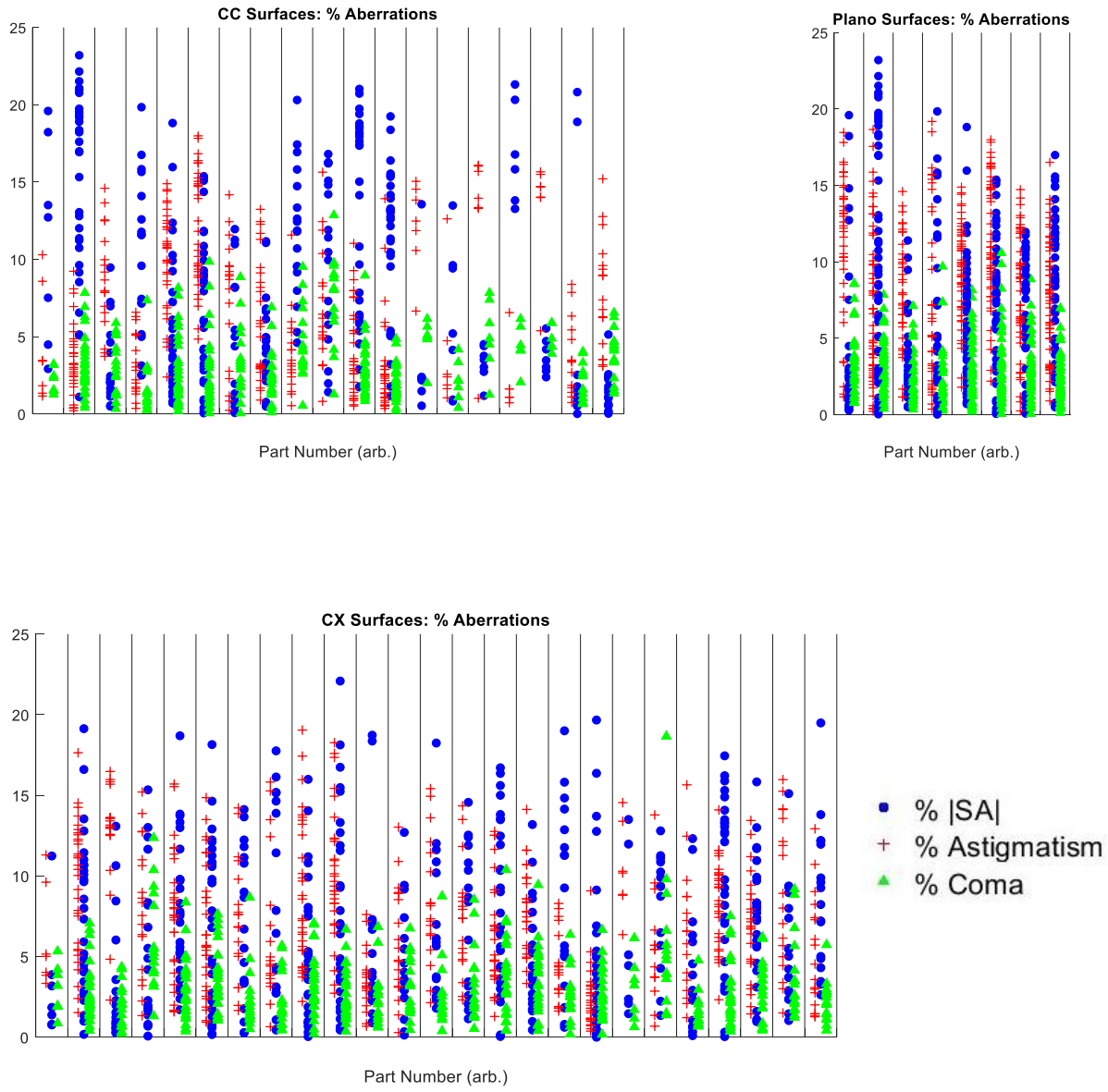

Figure 7. Plots of the percentage of contributions of spherical, coma, and astigmatism coefficients for concave (CC), convex (CX), and plano surfaces.

2.3 PV and rms

Next, the overall PV and rms values are examined to look for trends and to compare to other well-known rules of thumb. As shown in Figure 8, many of the surfaces are below the 0.063 µm that corresponds to a λ/10 PV specification. Most of the surfaces in this study are specified with λ/10 PV. Surfaces that have higher PV had a different PV specifications. As shown, the histograms of the PV values are offset, especially for the CX and CC surfaces. The plano surfaces exhibit a normal distribution. The CX and CC surfaces show that the distribution is significantly shifted towards the specification value. This is due to the manufacturing process – it is difficult to achieve a zero or close to zero irregularity value and because polishing typically stops if the PV is within specification (if the other parameters are also within specification). There is no manufacturing advantage to continue to polish to achieve a lower PV value. In fact, it is generally a disadvantage because of the risk of scratching, going center thickness minus, or getting out of radius tolerance.

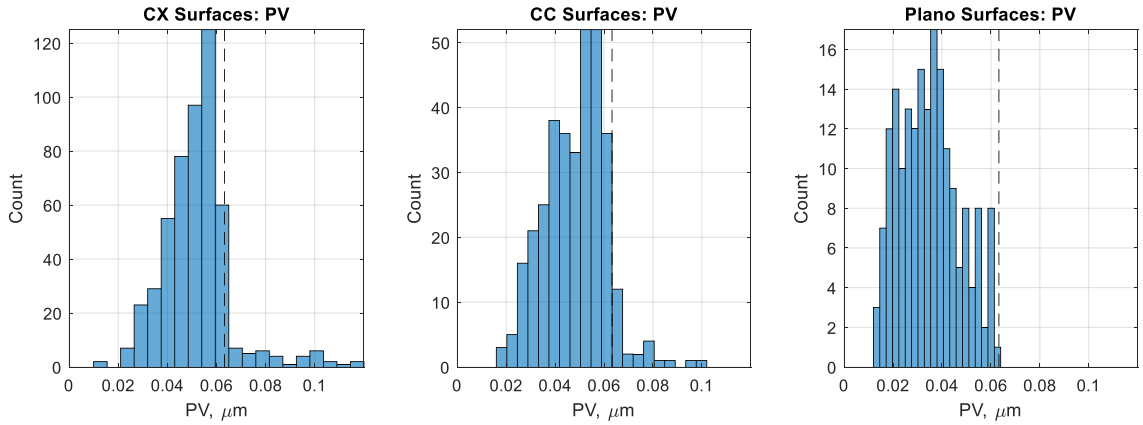

Figure 8. Histograms of the measured PV.

These histograms are often used to provide feedback to irregularity modeling. When tolerancing, the optical designer has the option of specifying what distribution to choose. Options vary between which software package is used, but they generally are normal (Gaussian), uniform, or parabolic. Based on the data in Figure 8, the designer should pick the parabolic distribution.

PV:rms Ratio

The "rule-of-thumb" ratio of PV to rms for an aberration varies greatly. The author has seen ratios ranging from 57:1 to 3:1. Overall, when cumulative aberrations in a surface error are considered, historical data shows a 5:1 ratio. This ratio is for traditionally polished surfaces with 'older' interferometers (i.e. lower pixel resolution). The PV:rms ratios of the measured surfaces in this report are shown in Figure 9 and Figure 10 (histogram). As shown, most of these surfaces have higher PV:rms ratios. Mean values are 6.2 for the CC surfaces, 7.5 for the CX surfaces, and 6.7 for Plano surfaces, which is not significantly larger than the rule of thumb. The difference may be explained by improved camera resolutions and noise in the measurement raising the PV, but not the rms.

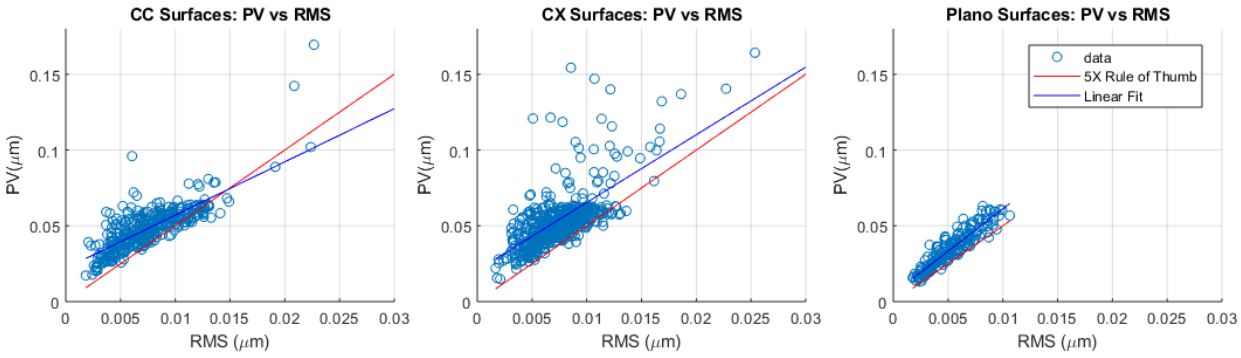

Figure 9. PV vs rms for all surfaces.

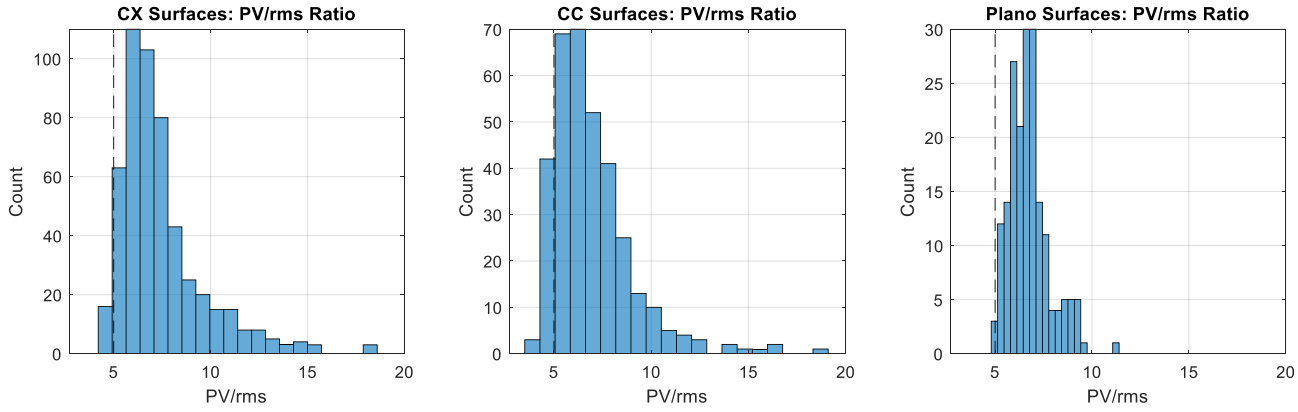

Figure 10. Histograms of the PV:rms ratio.

2.4 R/# Impact

Hypothesis #4 lists that the lens R/# has an impact on the propensity for a surface to have either spherical or astigmatism due to the ability for larger quantities of large R/# surfaces to be fabricated in parallel, while low R/# surfaces require individual tooling to be made. Figure 11 shows the aberrations plotted relative to the surface R/#. As shown, there does not appear to be a strong correlation in these data. The data also has a lack of sampling in certain ranges of R/#'s, but the distribution is relatively flat for the parts tested.

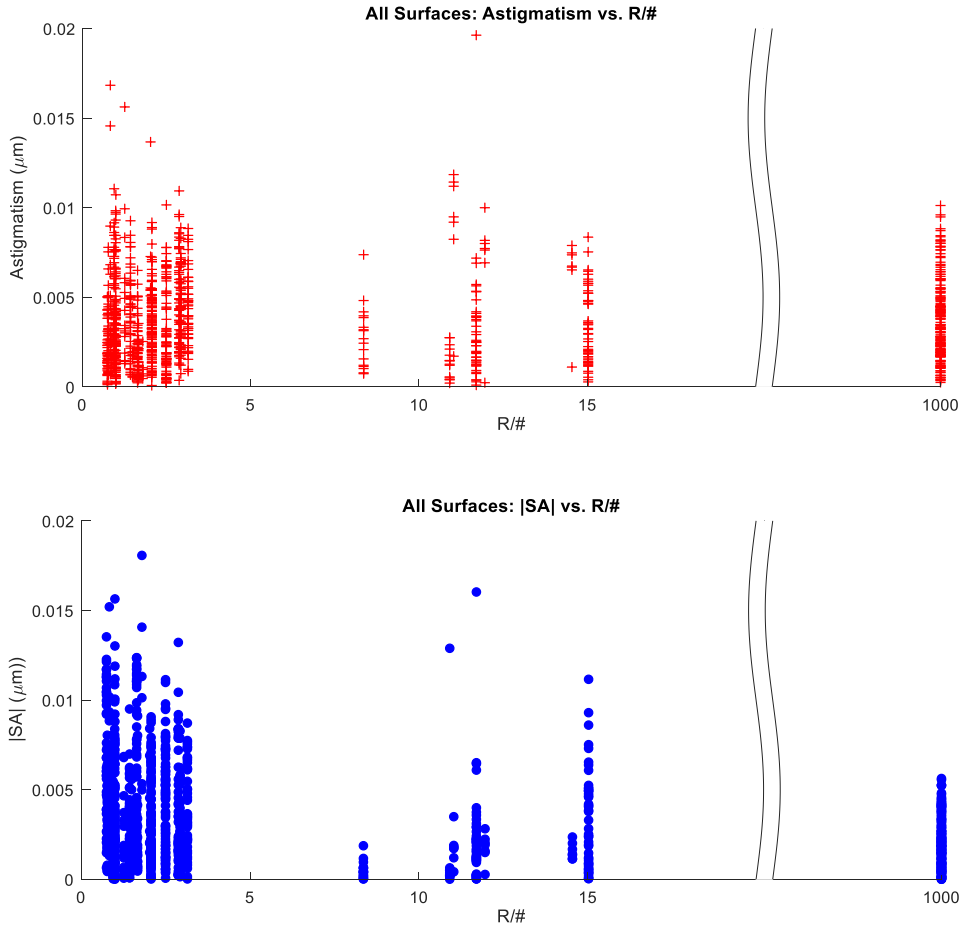

Figure 11. This plot shows coefficients measured for astigmatism and spherical in the fabricated lens surfaces with respect to the R/# of the given surface. Plano surfaces are represented by an R/# of 1000.

2.5 Lens Aspect Ratio Impact

Another hypothesis (#7) is the lens aspect ratio – specifically the ratio as defined by the lens center thickness divided by the physical outer diameter of the lens – could relate to the susceptibility of the optic to astigmatism. Again, there does not seem to be any obvious correlation between the lens aspect ratio and astigmatism or spherical. Figure 12 shows plots of the magnitude of spherical aberration, astigmatism, and coma versus aspect ratio for all lens data. These data are essentially independent of aspect ratio.

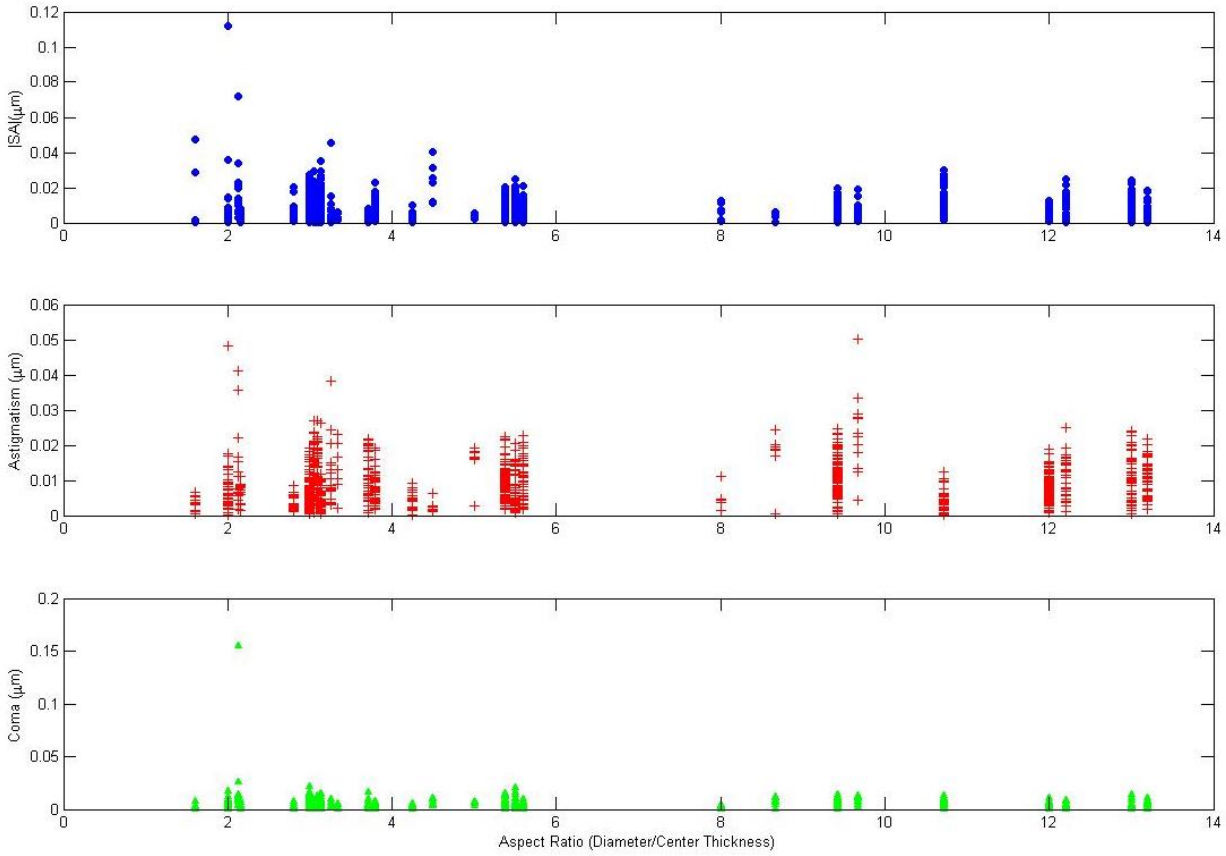

Figure 12. These plots show spherical aberration magnitude (top), astigmatism (center) and coma (bottom) for each lens aspect ratio. The similar distributions and relatively flat distribution across aspect ratios suggest little or no correlation exists between lens aspect ratio and any of these surface irregularities.

3. CONCLUSIONS

This report analyzes 1052 surface irregularity measurements of as-fabricated optical surfaces to compare to the optical model for TIRR and to known rules of thumb. One specific lesson learned during this analysis is the need for very close identification of which aberration definition is used (Zernike Fringe, Zernike Standard, vs. Seidel). The author has also found what appears to be an inconsistency in the TIRR analysis in Zemax showing that the PV of the modeled irregularity is not

the same PV that an optical manufacturer provides. It is also shown that the distribution of the PV errors should probably be modeled by a one-sided parabolic distribution.

The surface figure errors of spherical and astigmatism are not correlated, as some tolerancing and Monte-Carlo methods assume. While concave surfaces may have a negative correlation between the two figure errors, it is still not clear what lens design attributes may give rise to one over another as surface R/# does not seem to favor one type of figure error over the other. If it can be known which figure errors or what ratio of figure errors an optic is most likely to exhibit upon fabrication, those errors can be simulated during the Monte-Carlo analysis to grant a more accurate statistical yield of the as-built systems. In Zemax and OpticStudio, for example, instead of using the TIRR operand to perturb each surface with a random, but equivalent amount of spherical and astigmatic surface departure, the surface could be defined as a Zernike phase surface and the Zernike term and magnitude could be narrowed down to simulate a random amount of only those terms which that particular lens surface is known to be susceptible to during fabrication.

The hypotheses tested and the corresponding conclusions summarized in this work are as follows:

1) The amount of spherical aberration is not correlated to the amount of astigmatism.

   Conclusion: Confirmed. Figure 5 shows plots of spherical aberration vs astigmatism for concave, convex, and planar surfaces and it is evident that no correlation exits between the two across all surface types. The manufacturing process for spherical surfaces does not intrinsically lend itself to producing an equal amount of spherical aberration and astigmatism.

2) Convex and concave surfaces show no correlation between amounts of spherical and astigmatism.

Conclusion: Plausibly refuted. While the convex and planar surface types show no correlation between the spherical aberration and astigmatism the plot for concave surface suggests a weak negative correlation between spherical aberration and astigmatism.

3) Planar surfaces exhibit more astigmatism than spherical aberration.

   Conclusion: Confirmed. The plot for planar surfaces in Figure 5 clearly shows a smaller magnitude for spherical aberration than astigmatism.

4) Coma is lower in magnitude and not correlated to astigmatism.

   Conclusion: Confirmed. Figure 6 shows much smaller magnitudes for coma across all surface types. Since coma is an asymmetric function it stands to reason that it should occur in much smaller magnitudes than spherical aberration as the manufacturing process has rotational symmetries to produce spherical surfaces.

5) There is no correlation between the percentage of spherical, astigmatism, and coma on surface shape.

   Conclusion: Plausibly refuted. The plots for convex and planar surfaces in Figure 7 show a random distribution of spherical aberration and astigmatism percentages, but the concave surface depict a weak tradeoff between spherical aberration and astigmatism as the groupings for astigmatism percentage tend to be separated from the spherical aberration percentages in many parts.

6) There is a correlation between R/# and the amount of aberration.

Conclusion: Refuted. Despite a slight difference in manufacturing process for relatively small and large R/#'s which can logically be attributed to different aberrations, Figure 11 clearly shows there is no trend between R/# and surface spherical nor astigmatism for all surface types.

7) There is a correlation between lens aspect ratio and the amount of aberration.

   Conclusion: Refuted. Figure 12 shows there is no correlation or trend between lens aspect ratio and any of surface spherical aberration, astigmatism, nor coma.

4. FUTURE WORK

The spherical aberration considered here is as calculated from interferometric data fitting, which included higher order Zernike terms though they were not discussed in this work. Zernike terms are a convenient way to fit wave fronts and optical surfaces; however, it should be noted that there does seem to be a common surface deformation on optical surfaces that is rotationally symmetric, but is not described well by Zernike terms even when a large number of Zernike coefficients are considered. These lenses typically have some 'dimple' or 'bump' near the center of the aperture and often times a high 'lip' near the edge. It would be interesting to look in depth at the lens data and compare the disparity between these surfaces and their corresponding Zernike expansion fit as a result of these deformations, as well as model their impact on performance.

In the future, Ruda-Cardinal, Inc. would like to update previous Monte-Carlo analysis done for the systems using these optics with the as-measured distributions of surface errors and compare the expected performances of the perturbed systems to that of the as-built systems.

ACKNOWLEDGEMENTS

This research was done with the help of employees of Ruda Cardinal Inc.: Christopher M. Shanor, Isela D. Howlett, Kate Medicus, Tilman Stuhlinger, and Kenneth R. Castle, who are co-authors of this work which resulted in an SPIE publication and presentation. Ruda Cardinal Inc. would like to acknowledge the support of Optimax for providing the optical data analyzed herein.

REFERENCES

[1] Optimax Systems, Inc. https://www.optimaxsi.com/

[2] Zemax OpticStudio (version 16.5 SP5) [Raytrace software]. www.zemax.com

[3] Mahajan, V. N., “Zernike Polynomials and Wavefront Fitting,” in [Optical Shop Testing], ed. Daniel Malacara, John Wiley & Sons, Inc. Hoboken, New Jersey, (2007).

[4] Evans, C. J., “PVr-a robust amplitude parameter for optical surface specification,” Opt. Eng. 48(4) 043605 doi: 10.1117/1.3119307 (2009).

[5] Densmore, Victor, et al., "As-fab elements: design vs. reality," Proc. SPIE 10747, Optical System Alignment, Tolerancing, and Verification XII, 107470G (19 September 2018).